SAND--90-1003C

DE90 017042

ION COUPLING EFFICIENCY FOR AN EXTRACTION APPLIED-B ION DIODE ON THE HELIA LINEAR INDUCTION ADDER IN POSITIVE POLARITY*

D. L. Hanson, M. E. Cuneo, P. F. McKay, R. S. Coats, S. E. Rosenthal,
J. R. Chavez, W. F. Stearns, C. E. Heath, W. G. Adams, J. Ruscetti

Sandia National Laboratories, Albuquerque, New Mexico 87185 USA

Abstract

We report on initial experiments to investigate coupling of the four-stage HELIA linear induction accelerator (3.6 MV, 180 kA, 30 ns FWHM) to a uniformly insulated applied-B ion diode in planar extraction geometry. Extraction of an annular ion beam along the diode axis for ion transport and focusing experiments requires that HELIA operate in positive (reverse) polarity, where each of the four cathode voltage adder sections contributes a group of electrons of unique energy and canonical angular momentum to electron flow in a magnetically insulated transmission line (MITL). We show that a number of requirements must be met for efficient production of a uniform high intensity ion beam. An appropriate insulating magnetic field geometry is needed to provide uniform insulation of the anode ion emitting surface and reduce direct electron losses from the cathode MITL region to the anode. A flat diode impedance profile with $Z_D < Z_{SELF\text{-}LIMITED}$ is required for efficient MITL power coupling to the diode. Even when the MITL is efficiently insulated upstream of the diode, we observe that some flow (MITL sheath) electrons are lost directly to the anode along flux lines of the diode insulating magnetic field. These losses (amounting to about 10-20% of the total current) slightly reduce overall ion coupling efficiency compared to ion diodes with more conventional MITL power flow, but may also aid in the very rapid turn-on (< 6 ns) of dielectric flashover ion sources on this diode. In these experiments, we achieved ion coupling efficiencies I_{ION}/I_{TOT} of 60-70% at peak ion power and ion generation efficiencies I_{ION}/I_{DIODE} of 80-90% at peak ion power under optimum conditions. These ion efficiencies, if maintained on higher power extraction diodes, would be adequate for inertial confinement fusion (ICF) applications including a light ion driver module for the proposed Laboratory Microfusion Facility (LMF).

Introduction

High power light ion drivers for Inertial Confinement Fusion (ICF) must operate in extraction geometry, with ions accelerated along the diode axis. This allows channel transport, beam bunching, beam overlap, and target standoff for high power target experiments where multiple diodes must be used in parallel. Early extraction geometry ion diodes [1] were inefficient because the anode emitting surface was not uniformly insulated [2]. Recent experiments [2,3] with appropriate insulating magnetic field geometries have demonstrated high ion efficiencies, making extraction geometry diodes feasible for fusion applications. Because of ion source limitations and the self-magnetic field bending of high current density ion beams, high impedance drivers are required for the production of 100 TW ion beams. Technology for such high impedance drivers has been demonstrated in the 20 stage, 16 TW, 20 Ω Hermes-III linear induction accelerator [4] at Sandia National Laboratories. The conceptual design for a light ion driver for the Laboratory Microfusion Facility (LMF) [5] uses accelerator modules similar to Hermes-III to power extraction geometry applied-B ion diodes.

To support the development of a high impedance extraction geometry light ion driver module for LMF, we have studied the coupling of the four stage HELIA linear induction accelerator to a uniformly insulated applied-B extraction ion diode. Ion beam extraction requires that HELIA operate in reversed polarity with the inner conductor positive. In positive polarity, each of the four induction cavity voltage adder sections contributes a group of electrons of unique energy and canonical angular momentum to the electron flow in the MITL [6]. The performance of an adder MITL in positive polarity with an electron diode load has been investigated on both HELIA [7] and Hermes-III [8]. However, a magnetically insulated ion diode presents a more complex load to the accelerator than an electron diode. A key issue explored for the first time in these experiments is how this complex electron flow in the MITL couples into an applied-B diode, affecting anode turn-on and diode efficiency.

In this paper, we present experimental results concerned primarily with power flow coupling to the diode, including data on electron losses in the diode region, losses resulting from the interaction of MITL electron flow with the diode applied-B field, MITL losses upstream of the diode region, and their combined effect on ion efficiency. Particle-in-cell (PIC) simulations of electron flow in the diode feed region, using the MAGIC computer code, are in progress but are not yet available for presentation. The diode has also provided a testbed for active lithium source development and for the study of anode plasma evolution [9] and spectroscopy. Details of this work will be discussed elsewhere.

Experimental Arrangement

A schematic of the experiment is shown in Figure 1. The diode was powered by HELIA, a 4 stage linear induction accelerator [7,10] operated at about 3.6 MV, 180 kA in positive polarity for these ion diode experiments. The output of the final adder section is

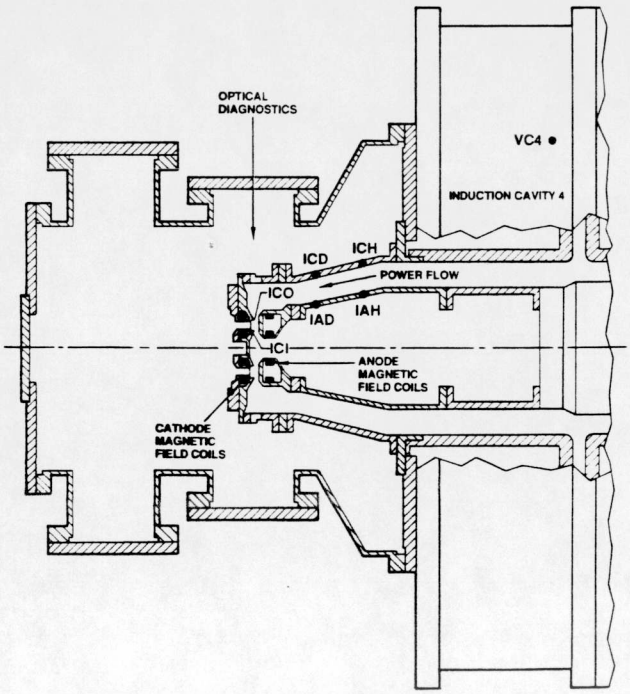

Figure 1. HELIA positive polarity applied-B extraction ion diode.

* This work is supported by the U. S. Department of Energy under Contract No. DE-AC04-76DP00789.

---

coupled to the extraction ion diode through a short straight (vacuum impedance $Z_0 = 22\ \Omega$, L = 42 cm) and a tapered ($Z_0 = 22$ to $26\ \Omega$, L = 19 cm) section of coaxial MITL. Initial experiments were performed with a 5-cm mean radius planar extraction ion diode using window screen and epoxy-filled grooved flashover anodes to produce an annular ion beam for vacuum transport along the diode axis. An anode-cathode (A-K) gap of 7.5 - 9.0 mm was used in all experiments. Electron flow across the diode gap was inhibited by the application of a strong radial magnetic field of between one and three Tesla. The insulating magnetic field geometry was accurately controlled using four anode and cathode field coils each driven by individual 60 kJ capacitor banks.

Electrical diagnostics included inductive cavity voltage monitors (VC1 - VC4) and paired common-mode-rejection B-dot loop current monitors in the cavities (IC1 - IC4) and in the tapered MITL section at positions H upstream of the diode (IAH, ICH) and D near the diode (IAD, ICD). Single loop B-dot ion current monitors ICO and ICI were located at the outer and inner cathode tips, respectively. These currents are used to define diode operating efficiencies. The **ion coupling efficiency** is defined as the ratio I_{ION}/I_{TOT} of the extracted ion current $I_{ION} \equiv II = ICO - ICI$ to the total accelerator current $I_{TOT} = IAH$ at peak ion power, where IAH is the anode MITL current measured farthest upstream from the diode. The **ion generation efficiency** is defined as the ratio I_{ION}/I_{DIODE} of the extracted ion current to the diode cathode current $I_{DIODE} = ICD$ at peak ion power. The diode voltage used to calculate ion power is determined by several techniques. In addition to the cavity voltage monitors, a 5-channel filtered Faraday cup array voltage diagnostic was located just behind the cathode tips. Techniques for deriving the diode voltage from MITL current measurements are described in the next section.

Ion beam diagnostics included witness plates, shadow boxes, Rutherford pinhole cameras, carbon nuclear activation samples, and a Thomson parabola. The dynamics of electron and plasma motion in the A-K gap were studied through measurements with a RING (Refractive INdex Gradient) diagnostic [9] and anode plasma spectroscopy. Work is in progress on improved diode voltage/beam energy diagnostics including an RFS (range-filter-scintillator) monitor and an ELV (electron-launching-voltage) monitor.

HELIA Diode Voltage Derived from Anode and Cathode Current Measurements

In this section, we will discuss appropriate methods for calculating the MITL voltage at the diode from anode and cathode currents. These methods are important since conventional resistive or capacitive voltage monitors are impossible to field on accelerators of this type, and voltage measurements are required to understand the diode operation in detail. As described above, voltages are also obtained directly from a filtered Faraday cup array diagnostic, and from capacitive voltage monitors in the inductive cavities, which are inductively corrected to yield an estimate of diode voltage. In a later section, we will compare directly measured and current-derived diode voltages in detail for a representative HELIA shot.

In the simple generalized flow (GF) model for a planar MITL, which is sufficiently accurate for our cylindrical MITL aspect ratio, the voltage across the MITL is given by [6,11]

$$V = Z_o \left(I_A^2 - I_C^2 \right)^{1/2} - \frac{m c^2}{2 e} \left(\frac{I_A^2}{I_C^2} - 1 \right) \qquad (1)$$

where Z_0 is the vacuum impedance of the MITL, I_A is the current in the anode line, I_C is the current in the cathode line, m is the electron mass, e is the electron charge, and c is the speed of light. Rosenthal [6] has shown that the GF model should not apply in the usual sense to positive polarity operation of HELIA and may result in an overestimate of the line voltage. This is because, at each adder stage, electrons are emitted into the flow (MITL sheath current) at a different cathode potential and with different canonical angular momentum, violating the assumptions of the model. He has proposed a method to calculate the positive polarity line voltage using the usual cathode current and a modified anode current that includes only electrons emitted into the flow by the last cathode. At cathode location i (i = 1-5 for HELIA), we have

$$V = Z_o \left(A^2 - B^2 \right)^{1/2} - \frac{m c^2}{2 e} \left(\frac{A^2}{B^2} - 1 \right) \qquad (2)$$

where $A = [(I_C)_i + (I_e)_i]$ and $B = (I_C)_i$. $(I_C)_i$ is the cathode current at i and $(I_e)_i$ is the component of flow current consisting of electrons emitted only from the i^{th} cathode, given by

$$(I_e)_i = [(I_A)_i - (I_C)_i] - [(I_A)_{i-1} - (I_C)_{i-1}]_{TS} \qquad (3)$$

where TS signifies that the waveforms at i - 1 are time-shifted ahead by the transit time separating the two positions. The assumption here, verified by simulations, is that upstream adder section electron flow does not affect the emission and flow of electrons from the final MITL cathode and therefore the relationship between $(I_e)_i$ and $(I_C)_i$ as a function of line voltage described by the simple theory is preserved. The flow originating from the last adder section and insulated during the main part of the pulse is called locally-emitted-flow (LEF).

Mendel [6] has shown that under more restrictive conditions, namely when the electron flow forms a uniform electron density that fills the MITL gap, the MITL voltage can be calculated using the usual anode and cathode currents without further assumptions about the energy or canonical momentum of the various components of that flow. The total electron flow in the MITL gap ($I_A - I_C$) is referred to as full gap flow (FGF), and the resulting line voltage is given by

$$V = \frac{Z_o}{2} \left(I_A^2 - I_C^2 \right)^{1/2} \qquad (4)$$

For steady state flow in an efficient MITL, the larger of the two voltages given by Eqs. (2) and (4) should be representative of the true voltage. If the LEF voltage exceeds the FGF voltage, it is likely that flow did not fill the whole gap. If the FGF voltage is larger, significant mixing of upstream adder section electrons with locally emitted electrons is indicated.

We performed GF, LEF, and FGF model calculations for a number of cases, and results are shown for a representative experiment in a later section. Where MITL operation was efficient, the LEF voltage was generally in reasonable agreement with other diode voltage measurements. The GF model typically overestimated the true diode voltage, while the FGF model underestimated the voltage, suggesting that electron flow does not fill the entire MITL gap for the low impedance, high efficiency shots considered.

Uniform Insulation and Electron Losses in the Diode Region

A number of factors affect the overall ion coupling efficiency I_{ION}/I_{TOT} of the diode, including efficient MITL operation, efficient confinement of diode electrons by the applied-B field, and rapid, uniform ion turn-on. In this section, we will be concerned with diode performance when the diode impedance throughout the power pulse is sufficiently low ($Z_D < Z_{SELF\text{-}LIMITED}$) to allow efficient MITL operation. Ion coupling efficiency will then be determined largely by electron losses within the diode region. The problem of electron flow and confinement within an applied-B ion diode on positive polarity HELIA is complicated by the interaction of flow electrons extending far out into the MITL feed gap with the diode applied magnetic field.

Slutz et al. have shown through PIC simulations and experimental work on low impedance extraction ion diodes [2,12] that uniform magnetic insulation of the anode emitting surface is one important requirement for high ion efficiency. The anode is insulated by a radial magnetic field to a voltage V_{CRIT}. For diode voltages $V < V_{CRIT}$, electrons emitted from the cathode that conserve their canonical momentum and energy are insulated from the anode. If V_{CRIT} varies across the anode emitting area, the spacing of the virtual cathode and resulting enhancement of ion current density over the Child-Langmuir space-charge-limited ion emission will vary across the anode. This variation in V_{CRIT} could result in overinsulated areas of the anode operating at lower enhancement or in underinsulated areas where electrons are lost, effects leading to reduced ion efficiency.

The magnetic flux distribution in the A-K gap required for uniform insulation of a cylindrically symmetric diode is given by [12]

$$\frac{\Delta \Psi}{r_A} = \frac{m c}{e} \left[\left(\frac{e V_{CRIT}}{m c^2} + 1 \right)^2 - 1 \right] \equiv G(V_{CRIT}) \qquad (5)$$

where $\Psi(r) = rA_\theta$ is the magnetic stream function, $\Delta\Psi = \Psi_A(r_A) - \Psi_C(r_C)$ is the difference between Ψ at the anode and the cathode, r_A and r_C are the radii of points on the anode and cathode, respectively, m is the electron mass, e is the electron charge, and c is the speed of light. In extraction geometry, the stream function at the anode Ψ_A

must vary with radius across the anode face as

$$\Psi_A(r_A) = G(V_{CRIT})\, r_A + \Psi_C \qquad (6)$$

In addition to providing increasing magnetic flux with radius in the A-K gap, the magnetic field geometry must also be designed to avoid flux surfaces which directly connect the anode with the cathode, along which electrons may be lost. V_{CRIT} values of 2.6 - 5.7 MV were used in these experiments.

Figure 2 shows a magnetic field profile satisfying the uniform insulation condition with the separatrix ($\Psi = 0$) at midgap. For the "non-gas cell" cathode configuration shown in Figure 2, the highest ion coupling efficiencies (60%) and most uniform anode ion emission (± 20% variation in proton charge over anode area) were achieved with a magnetic field geometry approximating this uniform insulation field profile. Lower efficiencies of 30-50% were obtained with the separatrix very near or penetrating the anode surface. This configuration may introduce electron losses along a flux line from a less insulated region of the cathode MITL to the anode.

We did observe that electron losses along the diode centerline had a significant effect on diode performance. Figure 3 shows a cathode configuration with indented cathode tips (to accept a gas cell window) and a centerline electrode gas seal which forms an electron emitting surface intersecting the diode and magnetic field symmetry axis. Electron losses along the diode centerline, measured with a Rogowskii coil behind the anode (Fig. 3), decreased from about 7-25% of ICD (bound current entering the diode) for the "gas cell" hardware to about 4% of ICD for a "modified gas cell" cathode with the centerline electrode removed.

Electron losses to the anode emitting surface were also enhanced with the centerline electrode present. For a "uniform insulation" magnetic field profile with the separtrix near midgap, witness plate and carbon activation measurements indicated ion emissions predominantly from the inner half of the anode surface. Uniform ion emission and high ion efficiencies could be obtained only by increasing the inner anode coil current to increase the insulation of the inner anode and move the separatrix away from the anode surface. Figure 4 shows the variation in ion coupling efficiency with inner anode coil current for a series of shots for fixed V_{CRIT}, HELIA Marx charge, and PFL (pulse forming line) gap spacing with the center electrode present. Optimum efficiency and beam uniformity were achieved by a 15-30% increase in inner anode coil current above the "uniform insulation" current.

To investigate the interaction of flow electrons with the diode applied magnetic field, we measured time-integrated electron losses to the anode MITL using 4-chlorostyrene radiochromic film

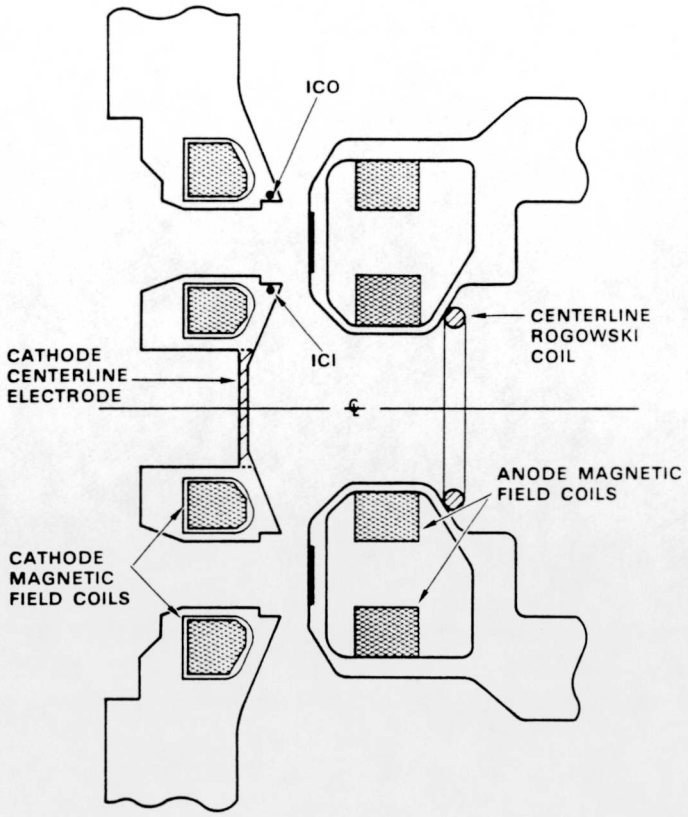

Figure 3. Detail of anode-cathode gap region showing centerline electrode present on unmodified "gas cell" cathode.

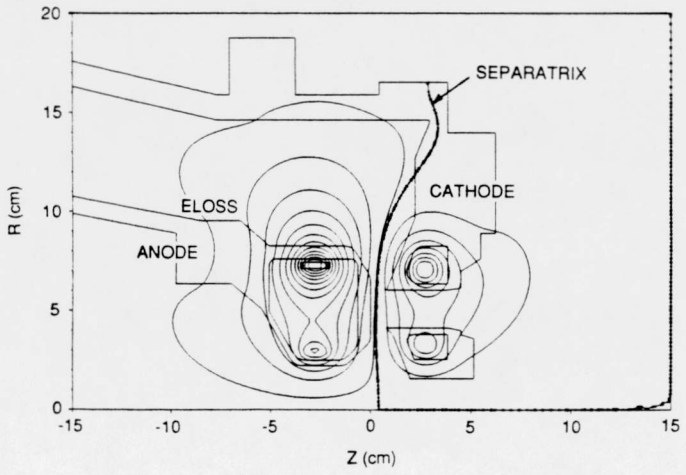

Figure 2. Uniform insulation applied magnetic field profile with separatrix near midgap.

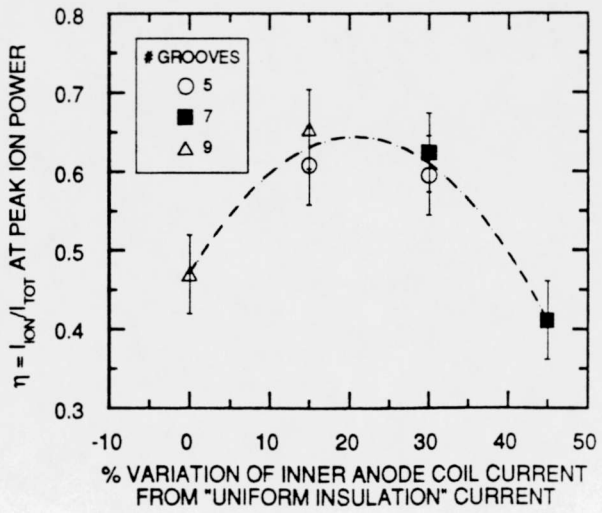

Figure 4. Variation of ion coupling efficiency with inner anode coil current.

detectors. We note that when the MITL is operating efficiently with a low impedance ion source, some electrons from the MITL flow are always lost to the anode at the point, labelled ELOSS in Figure 2, between the end of the aluminum (magnetic flux excluding) tapered MITL section and the stainless steel anode field coil support structure. At this location, the applied magnetic flux is concentrated and returned behind the anode. This loss probably occurs early in time, before the diode draws enough current to insulate the MITL flow past this point. As diode impedance is increased and magnetic insulation of the MITL is lost, electron losses are observed between the ELOSS location and locations progressively farther upstream, extending to the H position for the largest diode impedances. MAGIC PIC simulations will be performed in the future to study the time dependent electron flow in the diode and MITL regions and its interaction with the applied magnetic field in more detail.

Experimental Results for HELIA Shot 86

Figures 5 - 7 present experimental data for HELIA shot 86, a high power, high ion efficiency shot at a moderate V_{CRIT} of 3.6 MV ($V_{CRIT} < V_{OPEN\ CIRCUIT} \approx 5.4$ MV for 57 kV Marx charge) with a window screen flashover anode of area 41 cm^2. This is one of a series of high efficiency shots performed with a "modified gas cell" cathode with the centerline electrode removed (Figure 3) to reduce electron losses to the anode along the diode centerline. The diode impedance is sufficiently low throughout the power pulse to allow the MITL to operate with reasonable efficiency. Currents in the tapered MITL section are shown in Figure 5. Some loss of flow current to the anode at this high power level is indicated by the difference in anode currents IAH and IAD. Some retrapping of flow electrons in the cathode is also indicated by the increase in cathode current between the ICH and ICD monitors. Figure 6 shows the diode voltage determined by several different techniques. VD is the voltage at position D obtained from a lumped circuit model inductive correction of the summed cavity voltage waveform VCS = Σ VCi, i = 1-4 (Figure 7[a]). FFCA is the diode voltage measured by a filtered Faraday cup array using a time-resolved range-filter technique. Where an energy spread is present in the proton beam, this curve represents an upper limit on the diode voltage. GFM is the voltage at the diode calculated from the anode (IAD) and cathode (ICD) currents using the generalized flow model (Eq. 1) and overestimates the peak voltage because the conditions of the model are not met by the complex electron flow in positive polarity as discussed above. LEF is the voltage calculated using the locally-emitted-flow model (Eqs. 2 and 3) and appears to give a reasonable representation of the diode voltage. Finally, FGF is the voltage calculated using the full-gap-flow model (Eq. 6) and underestimates the diode voltage, indicating that flow electrons did not fill the entire gap on this shot.

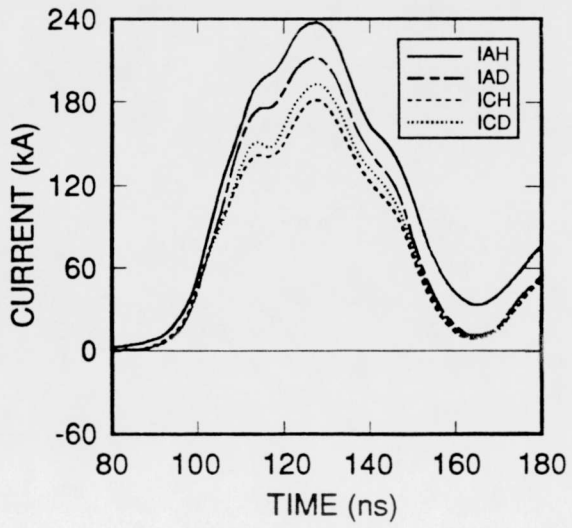

Figure 5. MITL currents IAH, IAD, ICH, and ICD for HELIA shot 86.

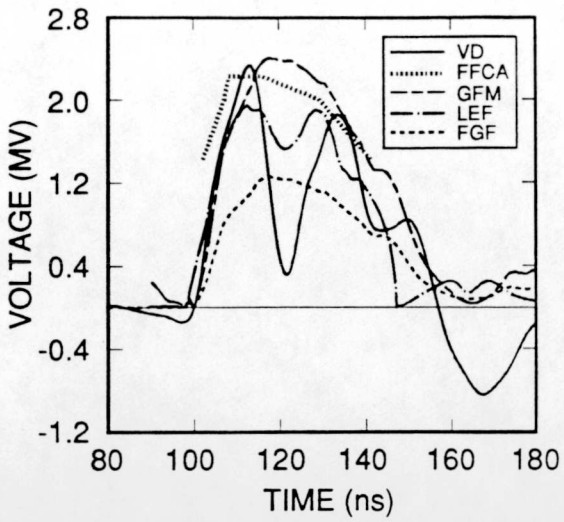

Figure 6. Comparison of measured and calculated diode voltages for HELIA shot 86: VD = inductively corrected voltage, FFCA = voltage determined from filtered Faraday cup array, GFM = voltage calculated from IAD and ICD using generalized flow model, LEF = voltage calculated from IAD, ICD using locally emitted flow model, and FGF = voltage calculated from IAD, ICD using full gap flow model.

Figure 7(a) shows the diode voltage and current waveforms for HELIA shot 86. VCS is the sum of the cavity voltage monitors. VD is a composite diode voltage waveform constructed from the data presented in Figure 6. ICD is the MITL cathode current at position D and II is the ion current. The ion turn-on time, defined as the time delay between the rise of the diode current and the rise of the ion current, is about 4.5 ns for this shot. We generally observe very short ion turn-on times for flashover anodes on this diode, ranging from 3 ns for low V_{CRIT} shots to 10 ns for shots with $V_{CRIT} > V_{OPEN\ CIRCUIT}$, with an average turn-on time for all shots of 5.7 ns. PIC simulations will be required to determine if flow current losses directly to the anode source region play a major role in this rapid ion turn-on. Fast ion source turn-on is essential for efficient coupling of diode energy into the ion beam. Ion power and energy determined using VD are shown in Figure 7(b). Total ion coupling efficiency was 70% and ion generation efficiency was about 90% on this shot. As shown in Figure 7(c), the ion diode load was undermatched to the driver with a relatively flat impedance profile throughout the power pulse.

Ion Efficiency vs. Diode Impedance

In our present configuration, the ion diode is close-coupled to the voltage adder section through a short MITL section. Because the MITL transit time is less than the rise time of the applied pulse, the load terminating the transmission line strongly affects the establishment of magnetic insulation. The efficiency of the line in turn strongly effects the overall ion coupling efficiency of the diode. To maintain insulation for a steady state magnetically insulated flow, the total current must exceed some minimum trapping current $I_{SELF-LIMITED} > I_{CRIT}$, where

$$I_{CRIT} = \frac{V}{Z_o}\left(\frac{F+1}{F-1}\right)^{1/2} \quad \text{with} \quad F = 1 + \frac{eV}{mc^2} \qquad (7)$$

is the critical current required to prevent a single electron preserving canonical momentum and energy from reaching the anode. When the load impedance reduces I_{TOT} below $I_{SELF-LIMITED}$, a loss of insulation will occur. The ion diode represents a dynamic load for the driver-MITL system. The impedance behavior of an applied-B diode depends on both the properties of the ion source and the motion of the virtual cathode, which is driven toward the anode by diamagnetic electron sheath currents [13] and controlled in part by the insulating magnetic field geometry.

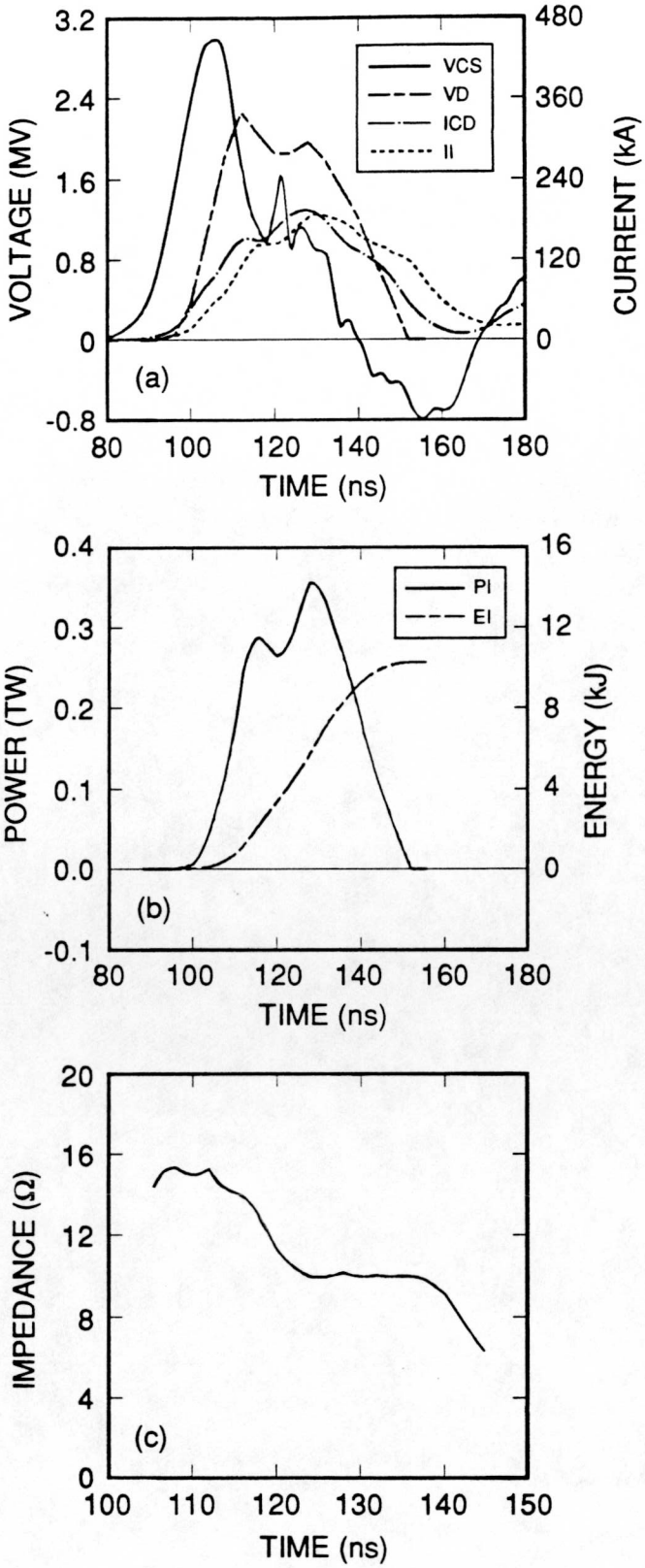

Figure 7. Diode performance for HELIA shot 86. a) Diode voltage, current waveforms: VCS = summed cavity voltage, VD = composite diode voltage waveform, ICD = diode current, II = ion current. b) PI = ion power, EI = ion energy. c) Diode impedance ZD = VD/ICD.

Figures 8 - 10 illustrate the effect of different diode impedance profiles on the MITL behavior upstream of the diode. These shots were all performed with a fixed HELIA Marx charge (40 kV) and PFL switch gaps, and at an A-K gap of 9 mm. On HELIA shot 71, the diode was uniformly insulated to a relatively low V_{CRIT} of 2.6 MV and the grooved epoxy anode turned on rapidly in 3.7 ns. This resulted in a low, relatively flat impedance profile throughout the power pulse (Figure 8[a]), producing efficient self-magnetically insulated operation with no MITL current losses near peak current (Figure 8[b]). The diode operated at an ion coupling efficiency 60%. The ion source on HELIA shot 74 (V_{CRIT} = 2.6 MV) was a window screen anode heavily coated with Eastman 910 adhesive. This anode turned on very slowly, resulting in a rapidly falling impedance profile (Figure 9[a]). The MITL current waveforms (Figure 9[b]) indicate significant losses in both flow and bound current between positions H and D before the line became fully insulated near peak current. The diode operated at an ion coupling efficiency of 25%. On HELIA shot 77, the diode was highly insulated to V_{CRIT} = 4.6 MV (V_{CRIT} > $V_{OPEN\ CIRCUIT}$ ≈ 3.8 MV) and ion turn-on of the epoxy flashover anode was relatively slow (9 ns). The diode operated at low enhancement and high impedance throughout the power pulse (Figure 10[a]), resulting in large MITL current losses upstream of the diode (Figure 10[b]) and very inefficient energy coupling to the diode. Ion coupling efficiency was 10% .

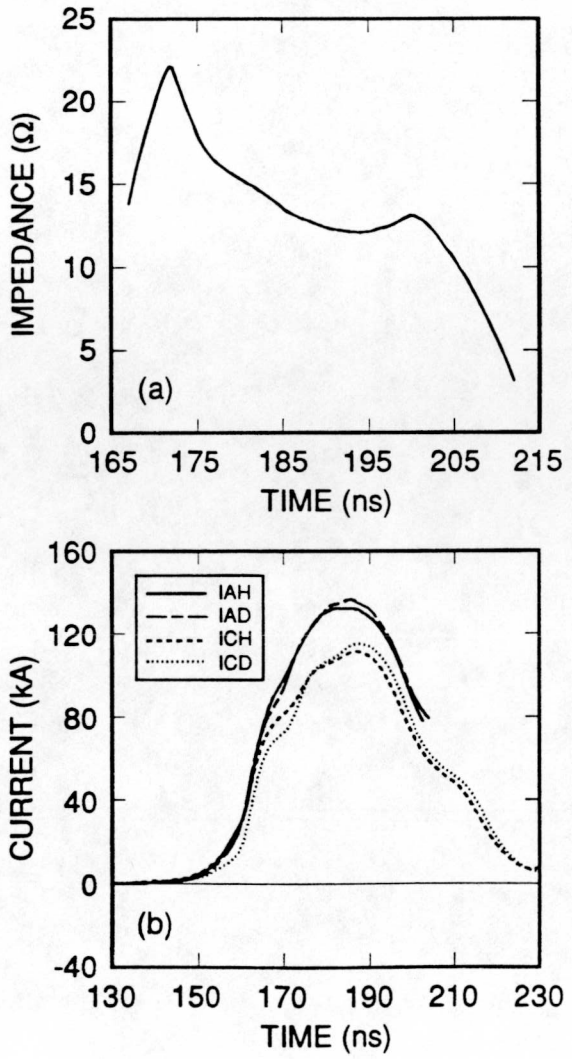

Figure 8. Diode impedance, MITL currents for HELIA shot 71 with 7 groove epoxy flashover anode at V_{CRIT} = 2.6 MV.

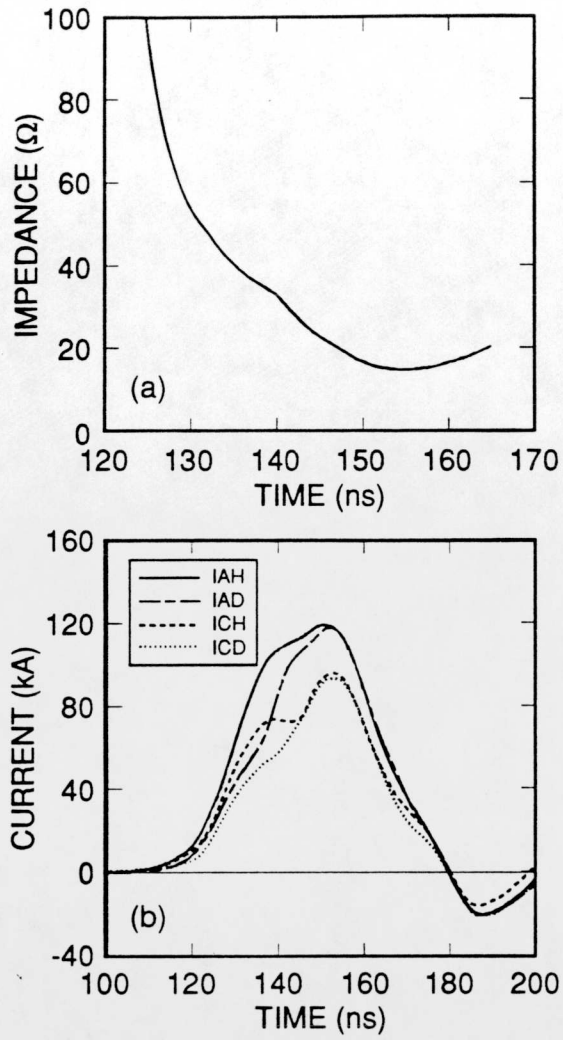

Figure 9. Diode impedance, MITL currents for HELIA shot 74 with coated window screen flashover anode at V_{CRIT} = 2.6 MV.

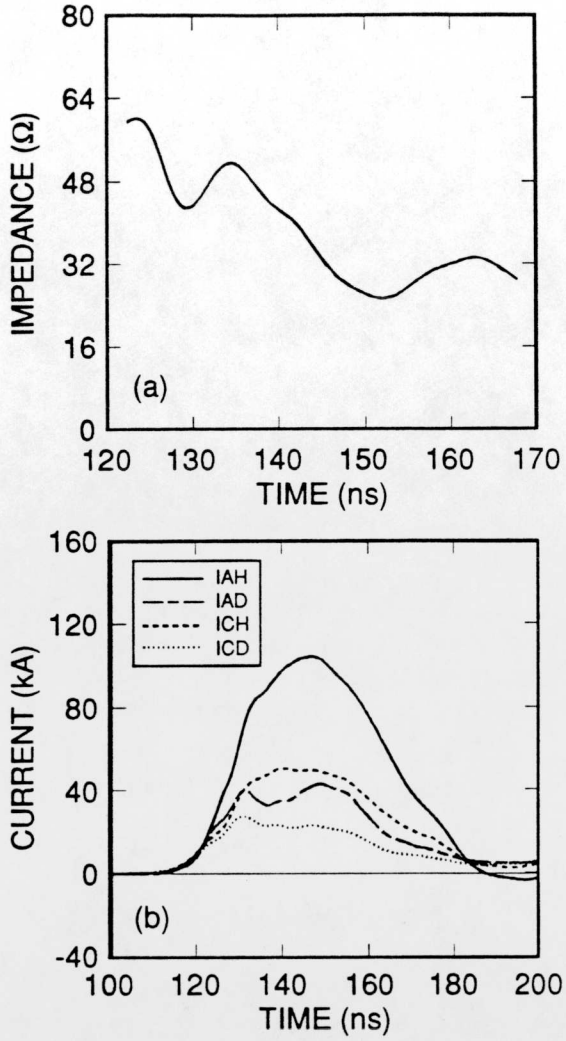

Figure 10. Diode impedance, MITL currents for HELIA shot 77 with 5 groove epoxy flashover anode at V_{CRIT} = 4.6 MV.

The effect of diode impedance on ion coupling efficiency is summarized in Figure 11 for a large number of medium (Marx charge 40 kV) and high power (Marx charge 58 kV) shots performed with several different cathode configurations and anode types. Where the diode operates at $Z_D < Z_{SELF\text{-}LIMITED} \cong 16\Omega$, current losses in the MITL are minimized and energy transfer to the diode is efficient. Ion coupling efficiencies are in the range of 50-70%, with variations resulting from differences in source behavior and details of electron loss in the diode region, as described earlier. Diodes featuring "gas cell" cathodes (Figure 3) with the centerline electrode removed operated reproducibly with ion coupling efficiencies of 60-70% and ion generation efficiencies approaching 90%. These extraction geometry efficiencies are acceptable for ICF applications such as the LMF light ion driver module and might be improved by active retrapping of the flow electrons which represent a primary loss mechanism for the diode. As we make the transition to high diode impedances ($Z_D > Z_{SELF\text{-}LIMITED}$), insulation is lost and ion efficiency falls off rapidly with decreased energy coupling to the diode. Some low efficiency shots resulted from operation at high V_{CRIT} ($V_{CRIT} \geq V_{OPEN\ CIRCUIT}$) where overinsulation of the A-K gap limited motion of the virtual cathode and forced the diode to operate at low enhancement [13]. Other high impedance shots involved source-limited anode behavior at lower values of V_{CRIT}.

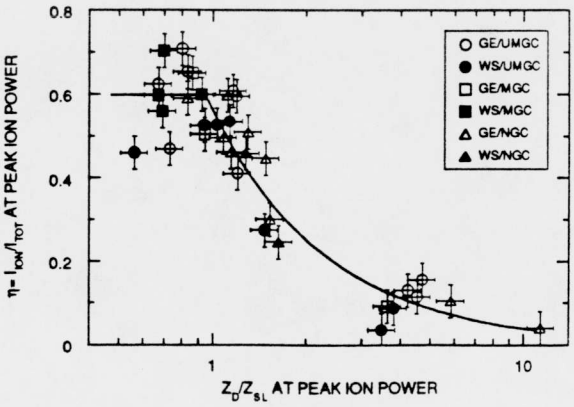

Figure 11. Ion coupling efficiency $\eta = I_{ION}/I_{TOT}$ vs. Z_D/Z_{SL} at peak ion power, where Z_D is the diode impedance and Z_{SL} is the self-limited line impedance (16 Ω). Anode types are: GE = grooved epoxy flashover anode, WS = window screen flashover anode. Cathode types are: UMGC = unmodified gas cell cathode with centerline electrode present, MGC = modified gas cell cathode with centerline electrode removed, NGC = non-gas cell cathode.

Conclusions

We have demonstrated the efficient operation of an applied-B extraction ion diode coupled to the HELIA linear induction accelerator operated in positive polarity. Peak ion coupling efficiencies of 60-70% and peak ion power levels of 0.3-0.4 TW have been achieved. For an extraction geometry diode with a high impedance driver in positve polarity, some flow electrons are lost directly to the anode along flux lines of the diode applied magnetic field. On HELIA, these losses are not prohibitive and may aid in the rapid turn-on of flashover ion sources. Otherwise, the requirements for efficient diode operation are similar to those for applied-B ion diodes on low impedance accelerators with more conventional MITL power flow. These include a flat diode impedance profile with $Z_D < Z_{SELF\text{-}LIMITED}$ for efficient MITL power coupling, uniform anode insulation for uniform ion beam production at maximum allowed enhancement, and an appropriate insulating magnetic field geometry to reduce direct electron losses to the anode and provide good electron confinement in the anode source region.

HELIA is currently being upgraded to SABRE, a 10 MV, 250 kA accelerator with ten linear induction cavities. We plan to continue extraction ion diode experiments with emphasis on gas transport of a neutralized beam, ion beam divergence measurements, ion source development, and improved power flow coupling into the diode for high voltage operation.

Acknowledgements

The authors would like to thank Drs. S. A. Slutz, D. J. Johnson, T. R. Lockner, and R. W. Stinnett for many useful discussions during the course of these experiments.

References

[1] D. J. Johnson, J. P. Quintenz, and M. A. Sweeney, "Electron and Ion Kinetics and Anode Plasma Formation in Two Applied Br Field Ion Diodes," J. Appl. Phys. **57**, 794 (1985).

[2] S. A. Slutz, D. J. Johnson, and J. T. Crow, "The Operation of a Uniformly Insulated Extraction Applied-B Ion Diode," submitted for publication.

[3] C. K. Struckman, B. R. Kusse, and G. Rondeau, Bull. Amer. Phys. Soc. **34**, 2064 (1989).

[4] J. J. Ramirez et al., "The HERMES-III Program," in Proceedings of the 6th IEEE Pulsed Power Conference,1987, p.294.

[5] D. L. Johnson et al., "A Conceptual Design for an LMF Accelerator Module," in Proceedings of the Particle Accelerator Conference, Chicago IL, March 1989.

[6] S. E. Rosenthal, "How to Calculate MITL Voltage on Positive-Polarity Hermes-III or HELIA," Sandia internal memo, February 15,1989.

[7] J. P. Corley et al., "Positive Polarity Voltage Adder MITL Experiments on HELIA," in Proceedings of the 7th IEEE Pulsed Pulsed Power Conference, 1989.

[8] D. L. Johnson et al., "Hermes-III Positive Polarity Experiment Experiment," in Proceedings of the 7th IEEE Pulsed Power Conference, 1989.

[9] M. E. Cuneo et al., "A Refractive INdex Gradient (RING) Diagnostic for Transient Discharges or Expansions of Vapors or Plasmas," these proceedings.

[10] T. W. L. Sanford et al., "Impedance of an Annular-Cathode Indented-Anode Electron Diode Terminating a Coaxial Magnetically Insulated Transmission Line," J. Appl. Phys. **63**, 681 (1988).

[11] C. W. Mendel, Jr., D. B. Seidel, and S. E. Rosenthal, "A Simple Theory of Magnetic Insulation from Basic Physical Considerations," Laser and Part. Beams **1**,311(1983).

[12] S. A. Slutz and D. B. Siedel, "Magnetic Insulation of Extraction Applied-B Ion Diodes," J. Appl. Phys. **59**, 2685 (1986).

[13] M. P. Desjarlais, "Theory of Applied-B Ion Diodes," Phys. Fluids **B1**, 1709 (1989).